Electronic Supplementary Information (ESI) for

Structural Diversity, Magnetic Properties, Luminescence Sensing of Flexible Tripodal Ligand of 1,3,5-Tris(4-carbonylphenyloxy)benzene Based Mn(II)/Cd(II) Coordination Polymers

Jie Zhang,[a] Liangqin Huo,[a] Xiaoqing Wang,[a] Kegong Fang,[b] Liming Fan,*[a] and Tuoping Hu*[a,b]

[a]*Department of Chemistry, College of Science, North University of China, Taiyuan 030051, China.*

[b]*State Key Laboratory of Coal Conversion, Institute of Coal Chemistry, Chinese Academy of Sciences, Taiyuan 030051, China.*

E-mail: hutuopingsx@126.com; limingfan@nuc.edu.cn.

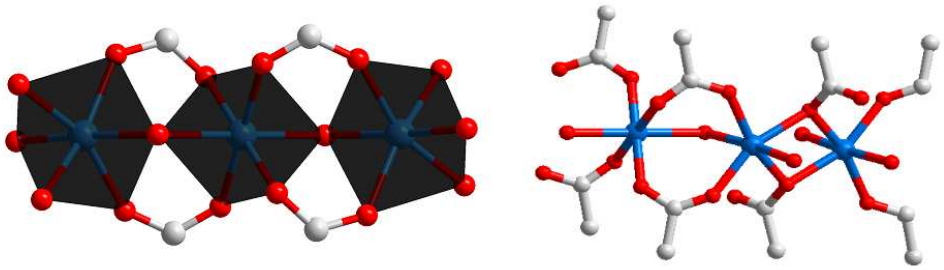

Figure S1. The different patterns of trinuclear $\{Mn_3(COO)_6(\mu_2\text{-}H_2O)_2\}$ SBUs in **1**.

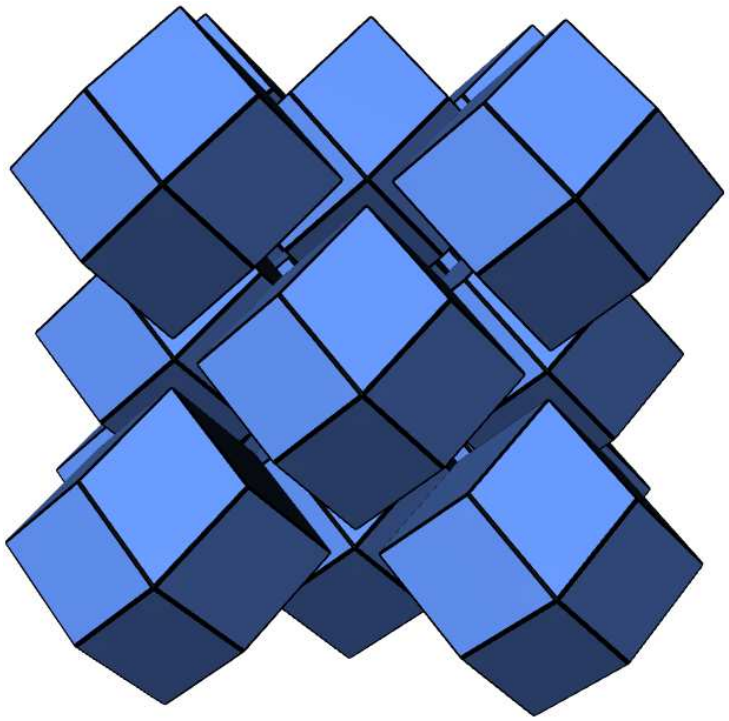

Figure S2. Tiling featured net of **1**.

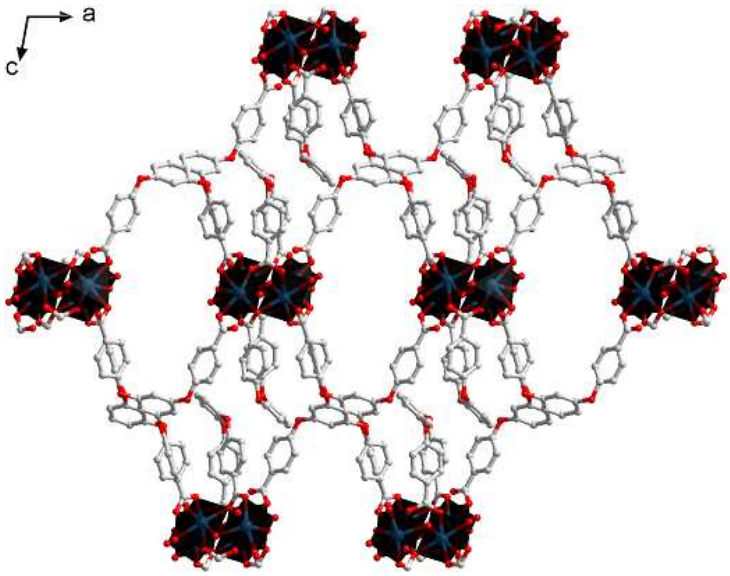

Figure S3. The 3D network constructed from two kinds of $TCPB^{3-}$ ligands coordinate with the 1D $\{Cd_6(COO)_8(\mu_3\text{-}OH)_2(\mu_2\text{-}OH_2)_2\}_n$ SBUs in **2** views along *b* axis.

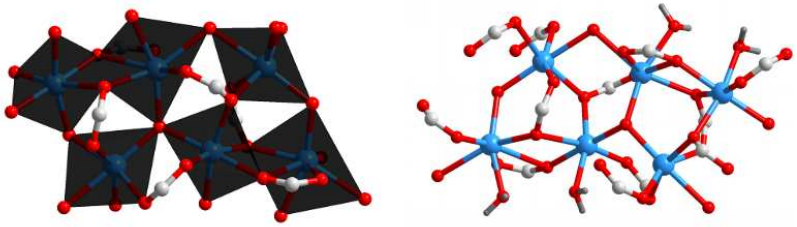

Figure S4. The different patterns of $Cd_6(COO)_8(\mu_3\text{-}OH)_2(\mu_2\text{-}OH_2)_2\}$ unit in **2**.

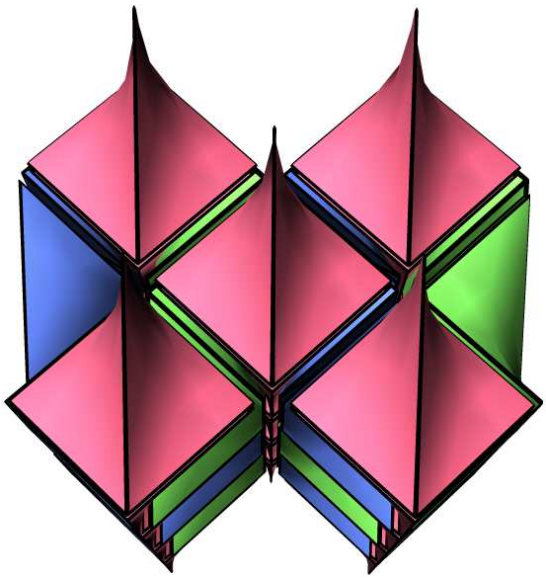

Figure S5. The tiling featured net of **2**.

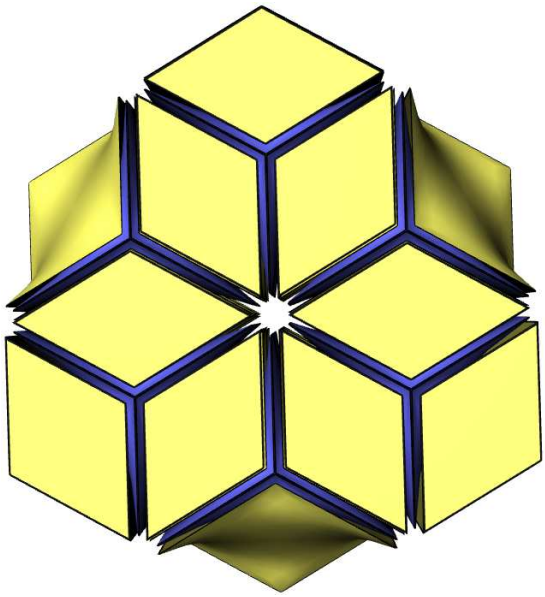

Figure S6. The tiling featured net of **3**.

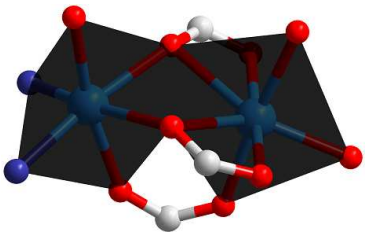

Figure S7. The binuclear $\{Cd_2(COO)_3\}$ SBUs in **4**.

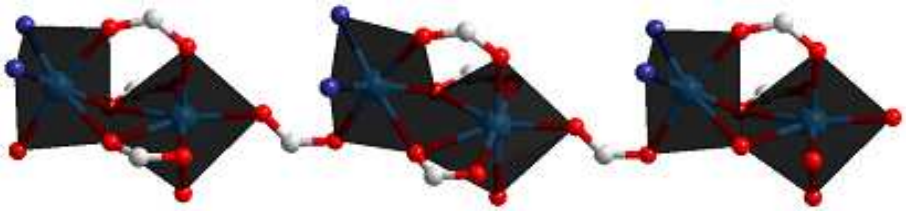

Figure S8. The 1D $\{Cd_2(COO)_2(HCOO)\}_n$ chain in **4**.

Figure S9. The 1D $\{Cd(bib)\}_n$ chain in **4** views along *a* axis.

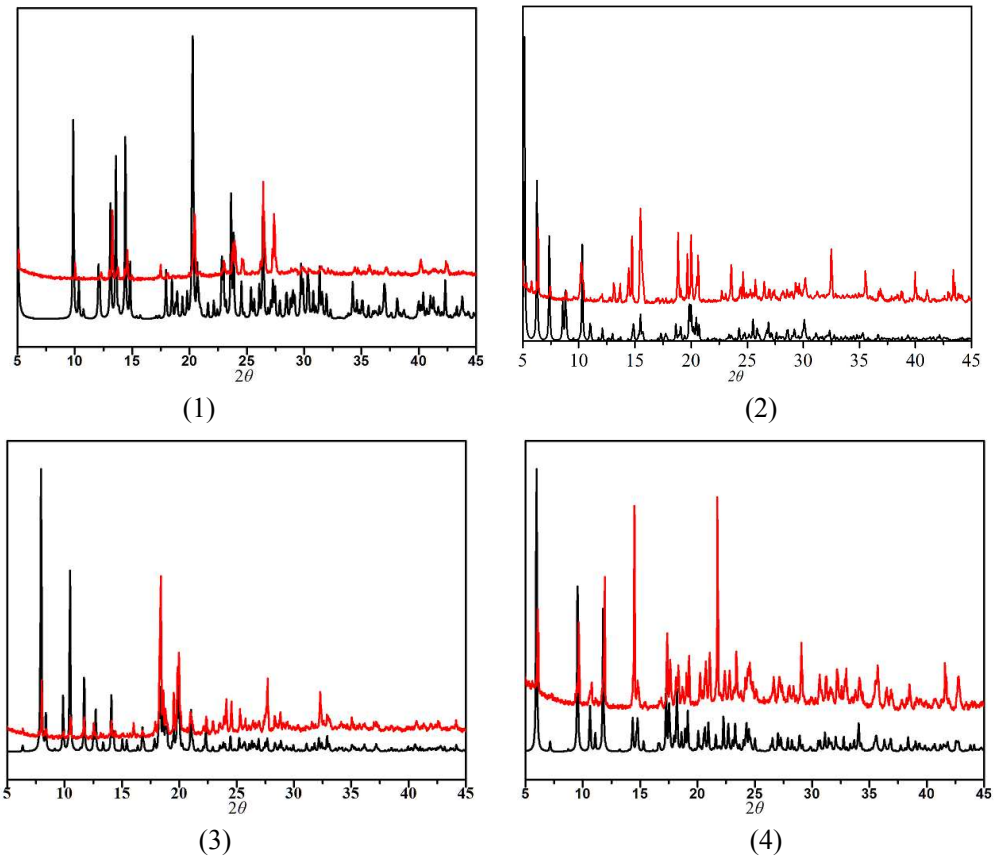

Figure S10. PXRD patterns of **1**-**4**. Dark: calculated from the X-ray single-crystal data; Red: observed for the as-synthesized solids.

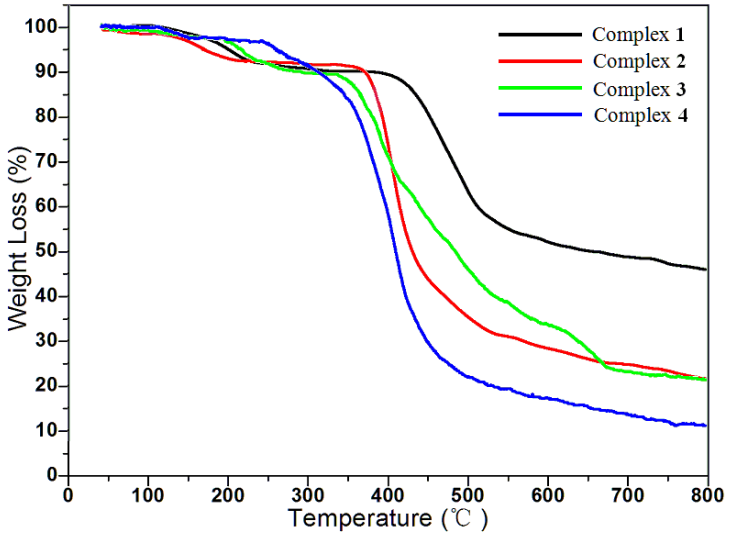

Figure S11. TGA curves for complexes **1**-**4**.

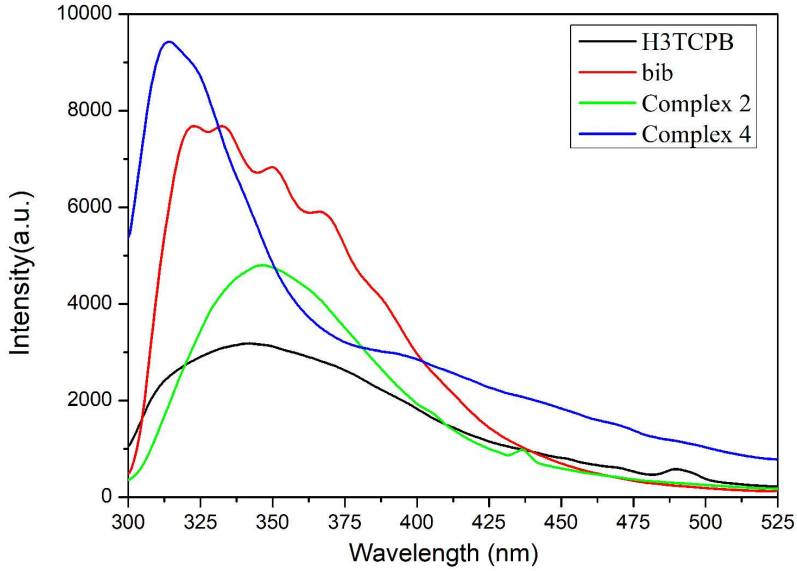

Figure S12. The fluorescence spectrum of organic linkers, complexes **2** and **4**.

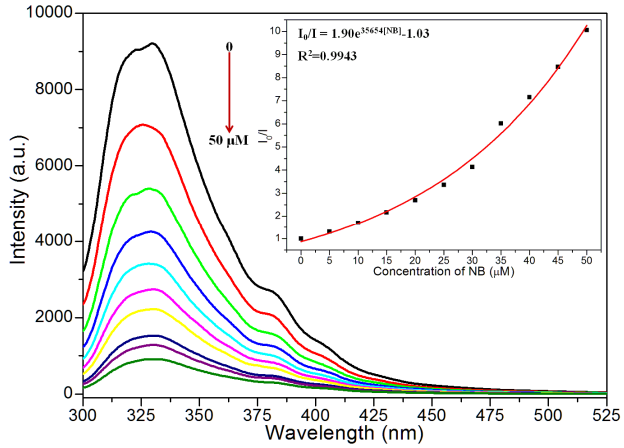

Figure S13. The PL spectra of the DMF suspension of **2** upon incremental addition of NB. Inset: The luminescent intensity (I_0/I) versus the nitroaromatics concentration.

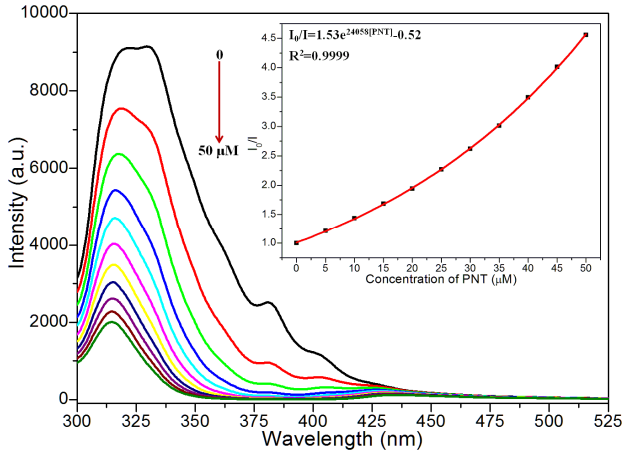

Figure S14. The PL spectra of the DMF suspension of **2** upon incremental addition of PNT. Inset: The luminescent intensity (I_0/I) versus the nitroaromatics concentration.

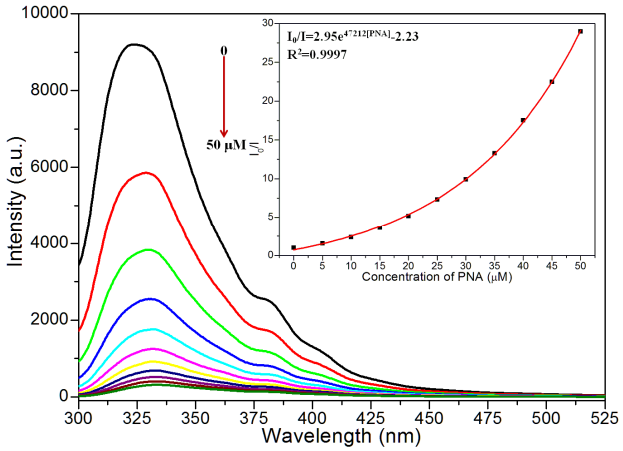

Figure S15. The PL spectra of the DMF suspension of **2** upon incremental addition of PNA. Inset: The luminescent intensity (I_0/I) versus the nitroaromatics concentration.

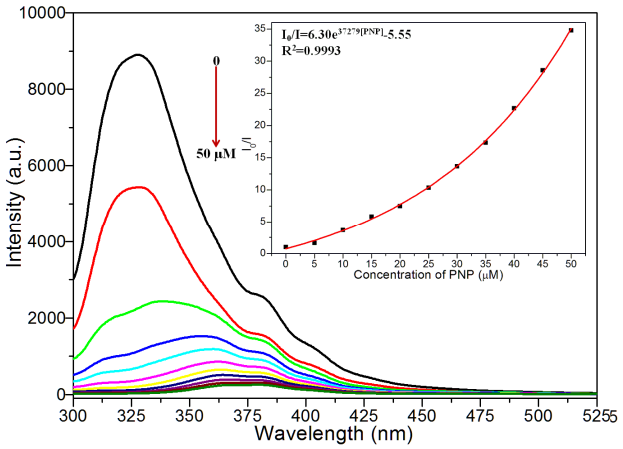

Figure S16. The PL spectra of the DMF suspension of **2** upon incremental addition of PNP. Inset: The luminescent intensity (I_0/I) versus the nitroaromatics concentration.

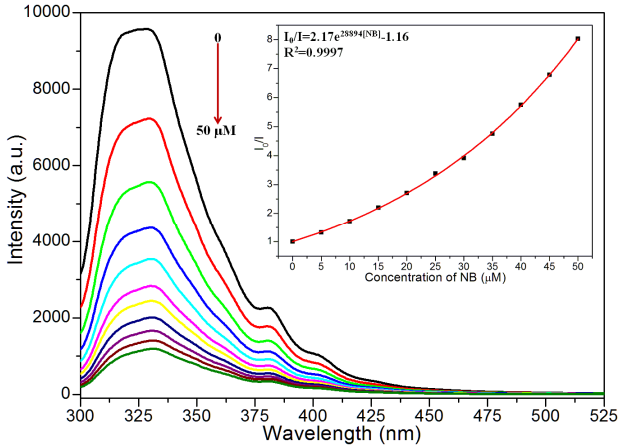

Figure S17. The PL spectra of the DMF suspension of **4** upon incremental addition of NB. Inset: The luminescent intensity (I_0/I) versus the nitroaromatics concentration.

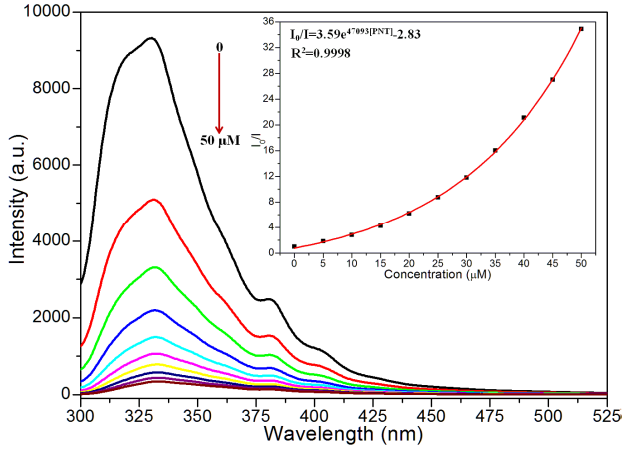

Figure S18. The PL spectra of the DMF suspension of **4** upon incremental addition of PNT. Inset: The luminescent intensity (I_0/I) versus the nitroaromatics concentration.

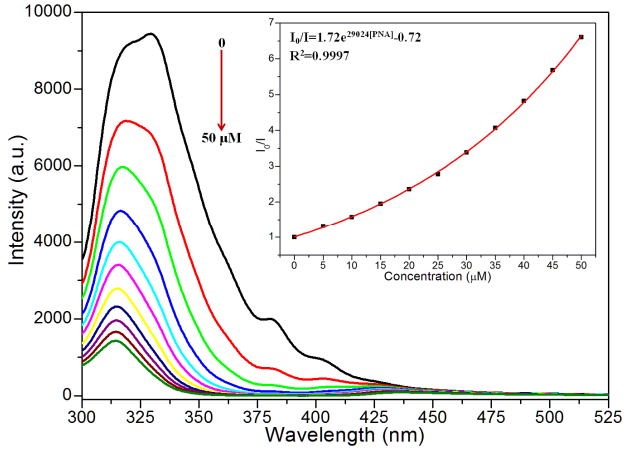

Figure S19. The PL spectra of the DMF suspension of **4** upon incremental addition of PNA. Inset: The luminescent intensity (I_0/I) versus the nitroaromatics concentration.

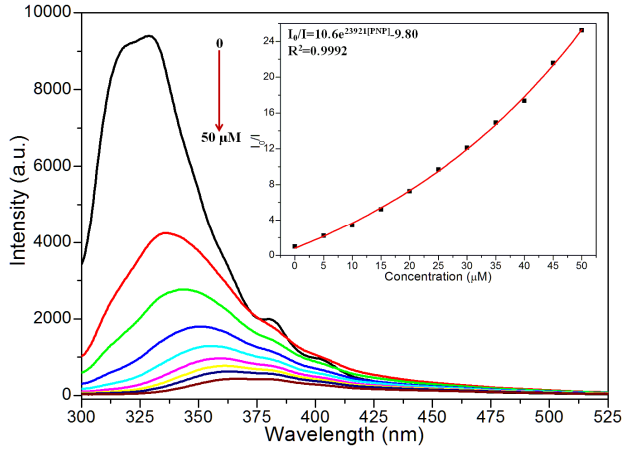

Figure S20. The PL spectra of the DMF suspension of **4** upon incremental addition of PNP. Inset: The luminescent intensity (I_0/I) versus the nitroaromatics concentration.

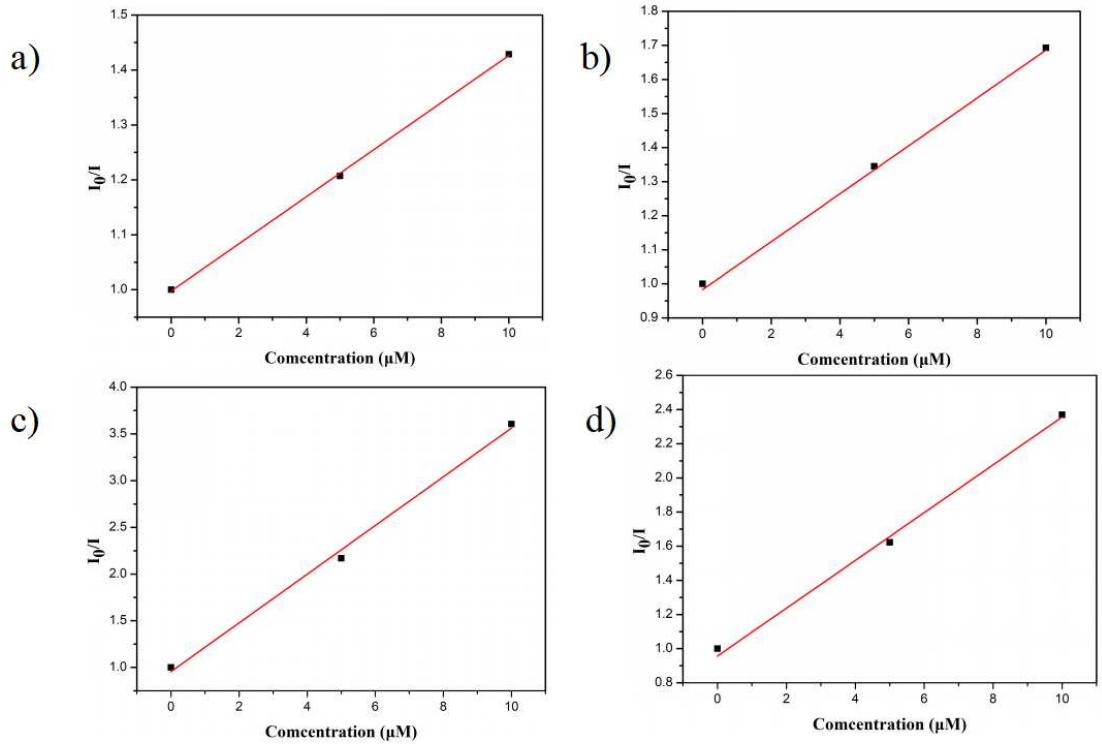

Figure S21. The linear plots at low concentration of PNT (a), NB (b), PNP (c) and PNA (d) for **2**.

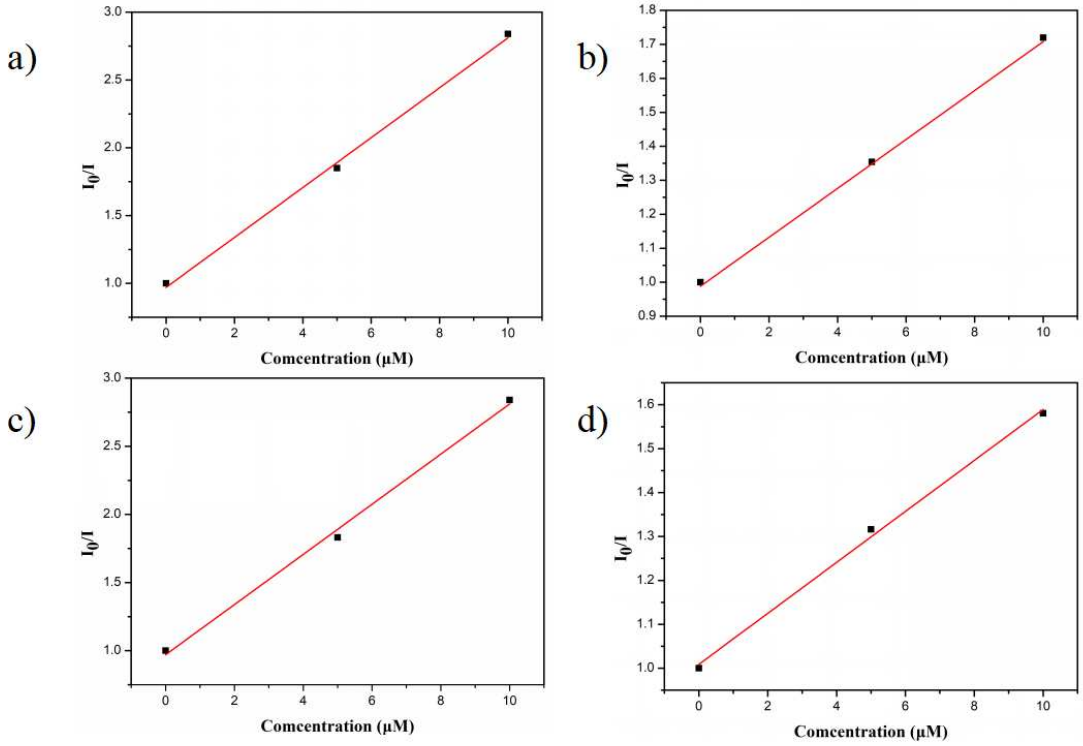

Figure S22. The linear plots at low concentration of PNT (a), NB (b), PNP (c) and PNA (d) for **4**.

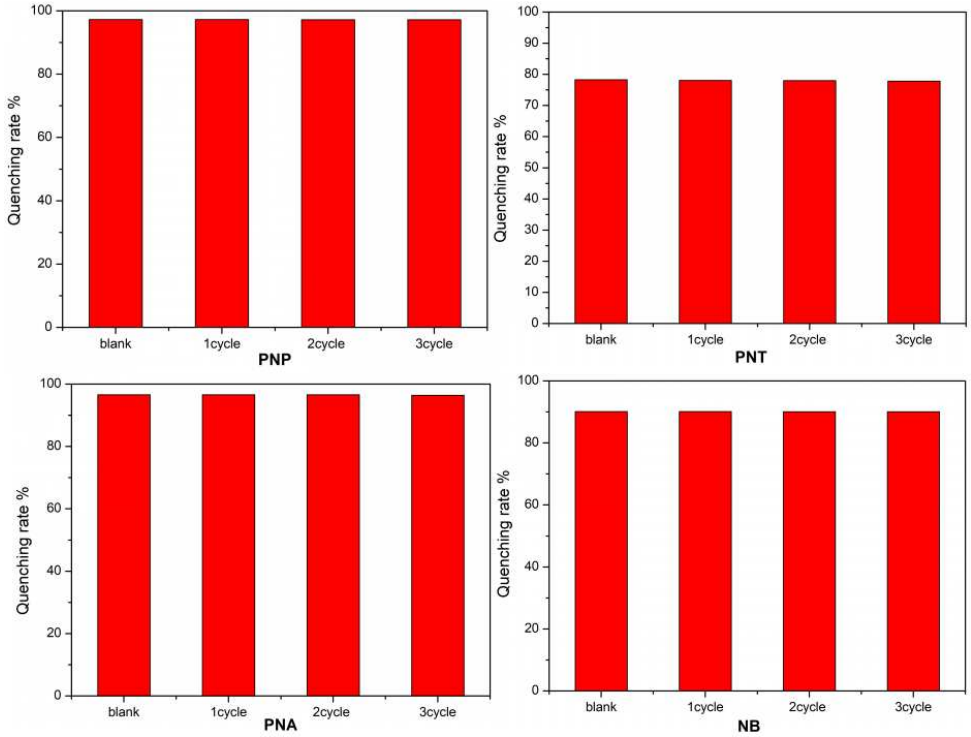

Figure S23. Fluorescence intensity ratio histograms of **2** for sensing NACs up to three cycles.

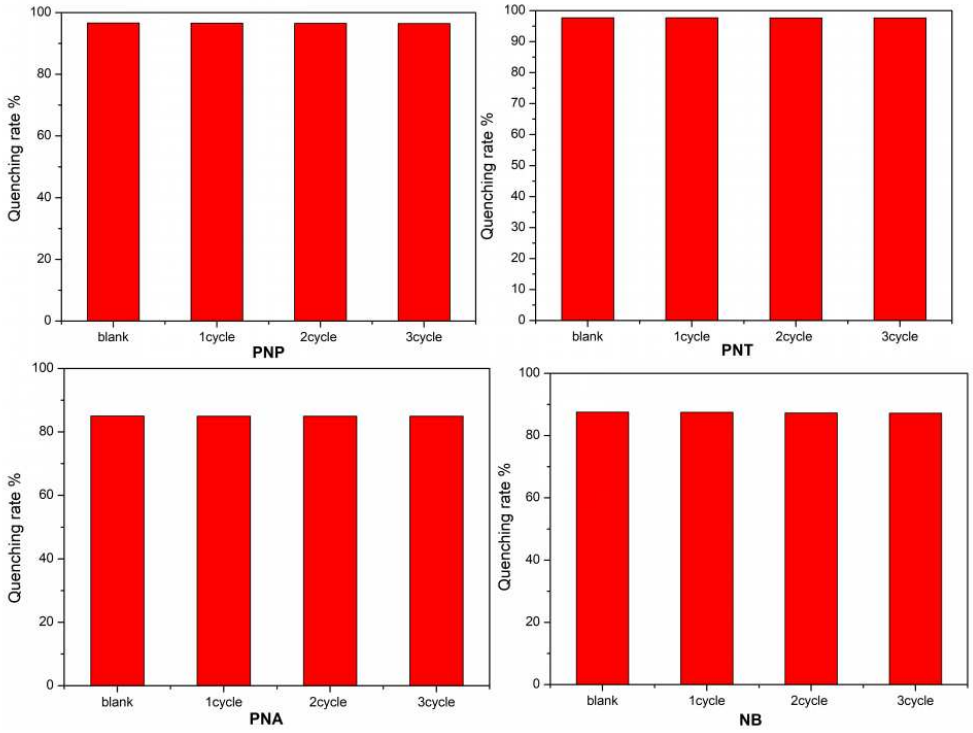

Figure S24. Quenching rate histograms of **4** for sensing NACs up to three cycles.

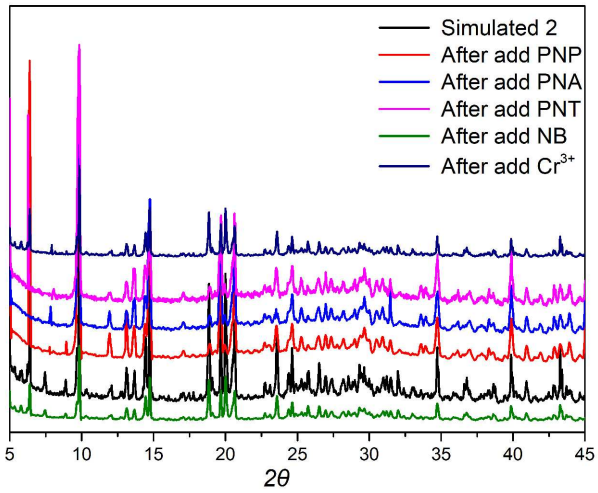

Figure S25. The PXRD pattern of **2** after immerging in several NAC-analytes and Cr^{3+}.

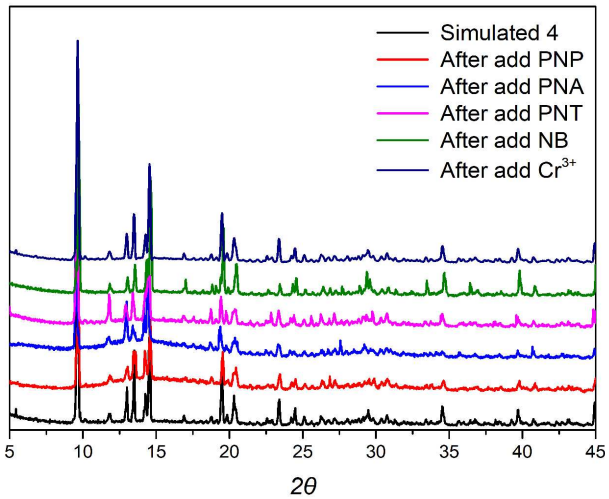

Figure S26. The PXRD pattern of **4** after immerging in several NACs and Cr^{3+}.

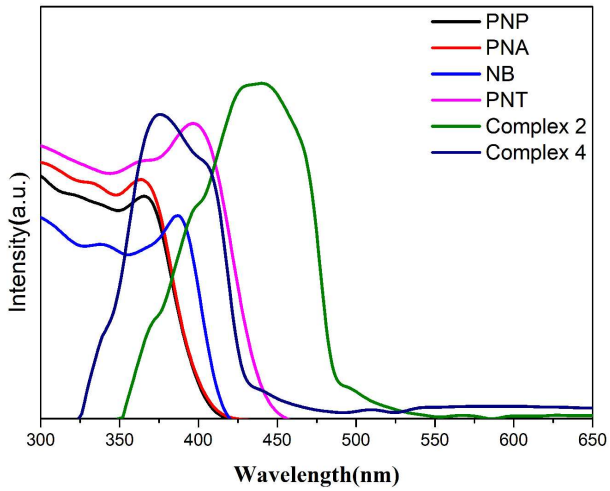

Figure S27. Spectral overlap between the normalized emission spectra of **2, 4** and normalized absorption spectra of NACs.

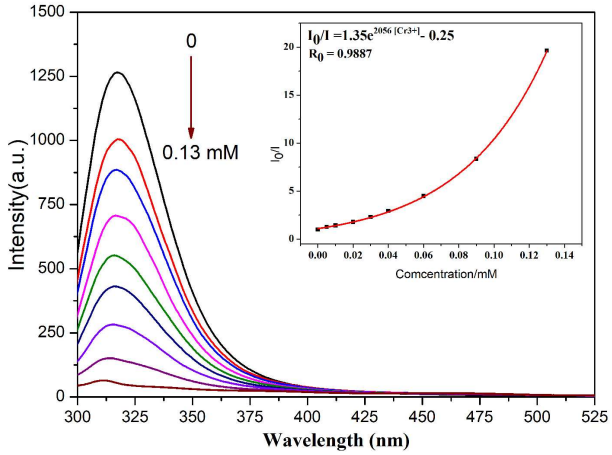

Figure S28. The PL spectra of the H_2O suspension of **2** upon incremental addition of Cr^{3+}. Inset: The luminescent intensity (I_0/I) versus the Cr^{3+} concentration.

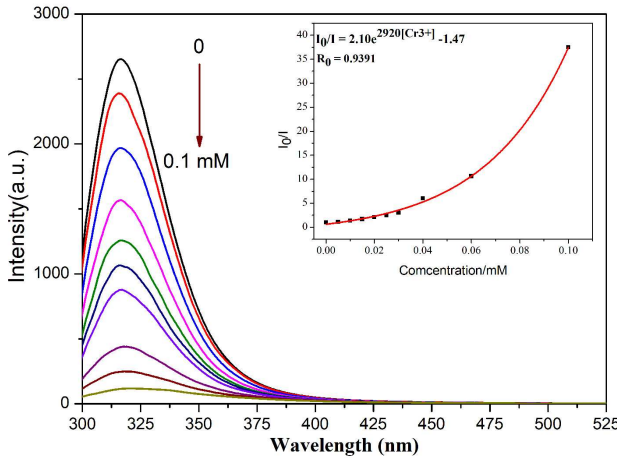

Figure S29. The PL spectra of the H_2O suspension of **4** upon incremental addition of Cr^{3+}. Inset: The luminescent intensity (I_0/I) versus the Cr^{3+} concentration.

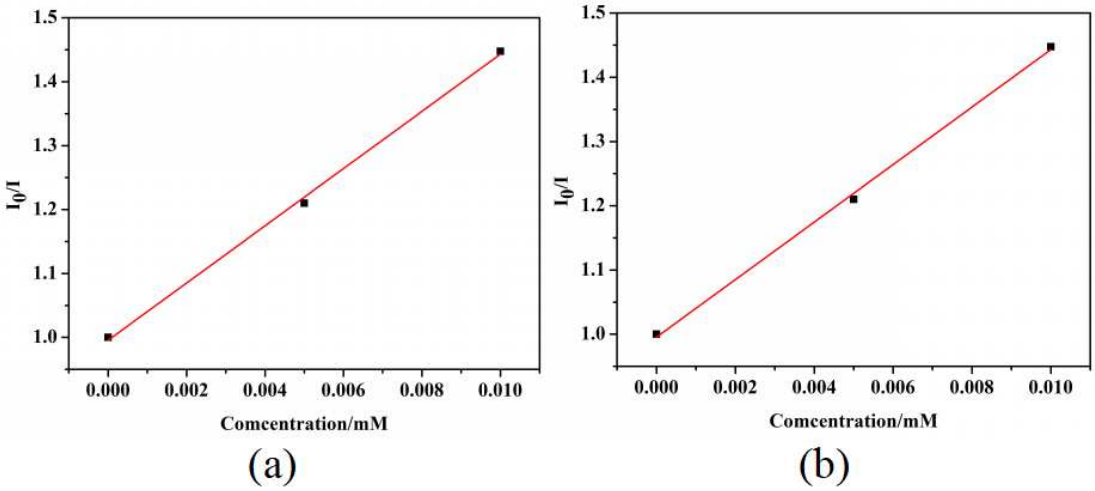

Figure S30. The linear plots at low concentration for **2** (a) and **4** (b).

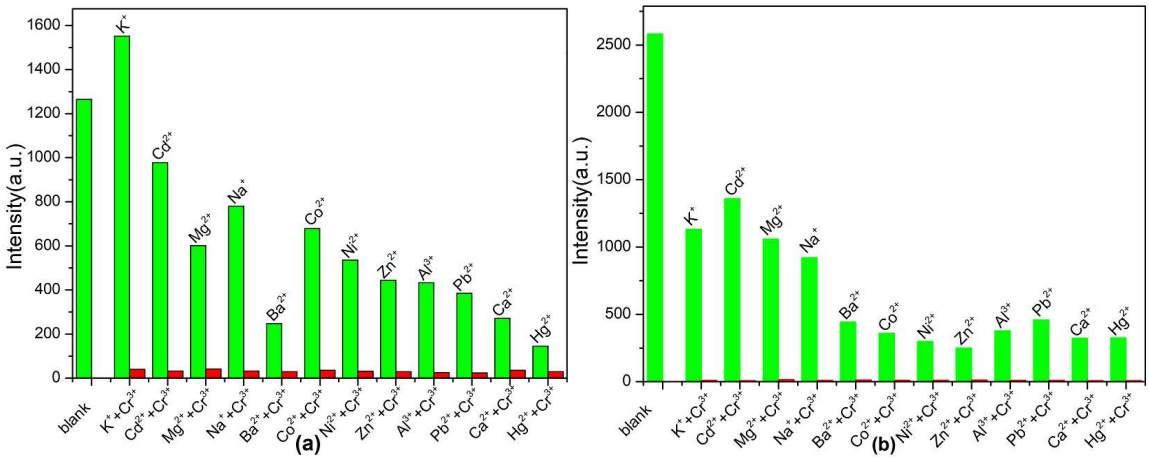

Figure S31. Comparison of the photoluminescence intensity of **2** (a) and **4** (b) in H_2O suspension with the 5 introduction of other metal ions (K^+, Cd^{2+}, Mg^{2+}, Na^+, Ba^{2+}, Co^{2+}, Zn^{2+}, Al^{3+}, Pb^{2+}, Ni^{2+}, Ca^{2+}, Hg^{2+}).

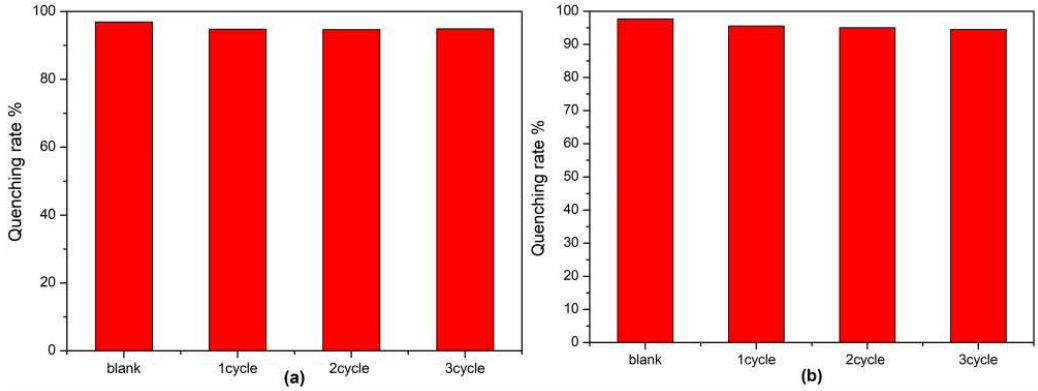

Figure S32. Quenching rate histograms of **2** (a) and **4** (b) for sensing Cr^{3+} up to three cycles.

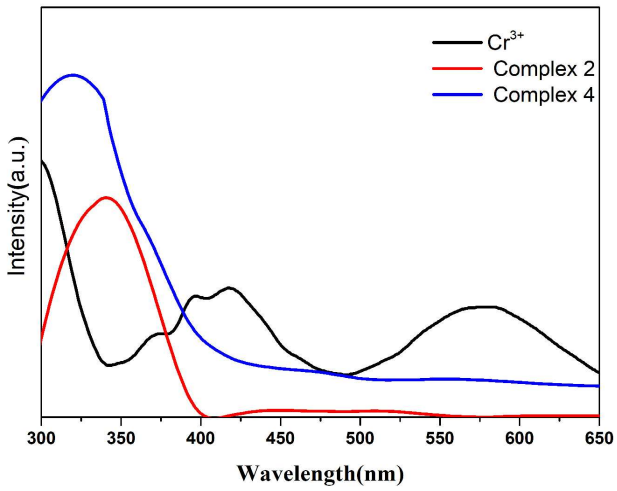

Figure S33. Spectral overlap between the normalized emission spectra of **2, 4** and normalized absorption spectra of Cr^{3+}.

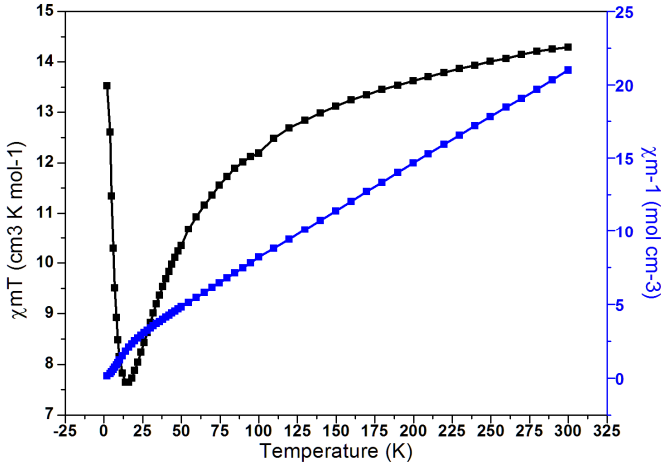

Figure 34. The temperature dependence of magnetic susceptibility of **1** under a static field of 1000 Oe.

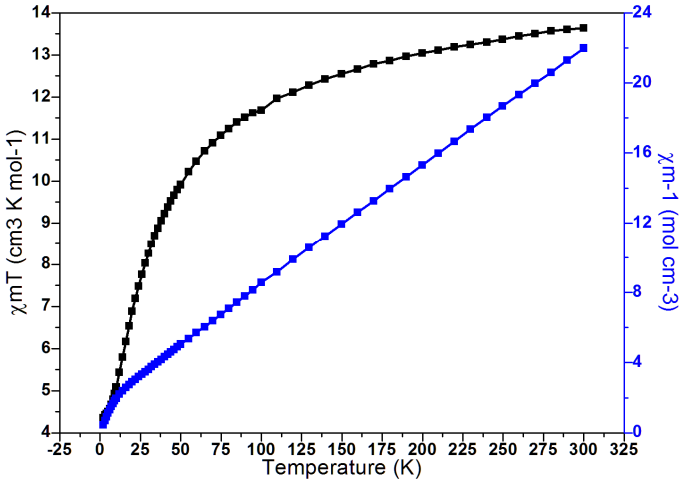

Figure 35. The temperature dependence of magnetic susceptibility of **3** under a static field of 1000 Oe.

Table S1 Crystal data for **1–4**

Compound	**1**	**2**	**3**	**4**
Empirical formula	$C_{54}H_{38}Mn_3O_{24}$	$C_{108}H_{80}Cd_7O_{47}$	$C_{72}H_{54}Mn_3N_6O_{20}$	$C_{42}H_{32}Cd_2N_4O_{13}$
Formula weight	1235.66	2916.59	1488.03	1025.54
Crystal system	Triclinic	Monoclinic	Triclinic	Monoclinic
Space group	*P*-1	*C*2/*c*	*P*-1	*C*2/*c*
a (Å)	7.8452(3)	28.6590(12)	10.9205(4)	26.1578(10)
b (Å)	9.0898(4)	11.4263(5)	11.1493(4)	18.5201(8)
c (Å)	18.4686(7)	34.8578(14)	14.4066(5)	17.6814(7)
α (°)	94.9263(12)	90	85.9620(10)	90
β (°)	100.8219(12)	100.3190(10)	75.3670(10)	109.4590(10)
γ (°)	108.0598(12)	90	87.4560(10)	90
V(Å^3)	1215.14(8)	11230.1(8)	1692.34(11)	8076.4(6)
Z	1	4	1	8
D_{calcd} (Mg/m^3)	1.689	1.725	1.460	1.687
μ(mm^{-1})	0.863	1.392	0.632	1.126
T(K)	293(2)	293(2)	296(2)	296(2)
F(000)	629	5760	763	4096
R_{int}	0.1312	0.0833	0.0867	0.1381
Final *R* indices[$I > 2\sigma(I)$][a]	$R_1 = 0.0600$, $wR_2 = 0.1476$	$R_1 = 0.0365$ $wR_2 = 0.0809$	$R_1 = 0.0658$, $wR_2 = 0.1831$	$R_1 = 0.0471$ $wR_2 = 0.1230$
R indices (all data)[a]	$R_1 = 0.0704$, $wR_2 = 0.1555$	$R_1 = 0.0700$, $wR_2 = 0.0868$	$R_1 = 0.0989$, $wR_2 = 0.2034$	$R_1 = 0.0600$ $wR_2 = 0.1352$
Gof	1.038	0.918	1.036	1.042

[a] $R_1 = \Sigma| |F_o|-|F_c| |/ \Sigma|F_o|$, $wR_2 = [\Sigma w(F_o^2-F_c^2)^2]/ \Sigma w(F_o^2)^2]^{1/2}$

Table S2 Selected bond lengths (Å) and angles (º) for **1-4**.

Complex **1**

Mn(1)-O(15)	2.149(2)	Mn(1)-O(1)	2.2147(19)	Mn(2)-O(3)	2.071(2)	Mn(2)-O(19)$^{\#4}$	2.193(2)
Mn(1)-O(10)	2.155(2)	Mn(1)-O(1)$^{\#1}$	2.2200(18)	Mn(2)-O(3)$^{\#2}$	2.071(2)	Mn(2)-O(7)$^{\#5}$	2.318(2)
Mn(1)-O(22)	2.159(3)	Mn(1)-O(7)	2.265(2)	Mn(2)-O(19)$^{\#3}$	2.193(2)	Mn(2)-O(7)$^{\#6}$	2.318(2)
O(15)-Mn(1)-O(10)	113.76(9)	O(22)-Mn(1)-O(1)$^{\#1}$	94.45(10)	O(3)-Mn(2)-O(19)$^{\#3}$	89.37(11)	O(15)-Mn(1)-O(7)	86.77(8)
O(15)-Mn(1)-O(22)	93.84(10)	O(1)-Mn(1)-O(1)$^{\#1}$	75.49(7)	O(3)$^{\#2}$-Mn(2)-O(19)$^{\#3}$	90.63(11)	O(10)-Mn(1)-O(7)	85.54(8)
O(10)-Mn(1)-O(22)	89.81(11)	O(19)$^{\#3}$-Mn(2)-O(7)$^{\#5}$	86.00(8)	O(3)-Mn(2)-O(19)$^{\#4}$	90.63(11)	O(3)-Mn(2)-O(7)$^{\#6}$	83.45(9)
O(15)-Mn(1)-O(1)	87.46(8)	O(19)$^{\#4}$-Mn(2)-O(7)$^{\#5}$	94.00(8)	O(3)$^{\#2}$-Mn(2)-O(19)$^{\#4}$	89.37(11)	O(3)$^{\#2}$-Mn(2)-O(7)$^{\#6}$	96.55(9)
O(10)-Mn(1)-O(1)	158.43(8)	O(19)$^{\#3}$-Mn(2)-O(7)$^{\#6}$	94.00(8)	O(1)-Mn(1)-O(7)	100.15(7)	O(1)$^{\#1}$-Mn(1)-O(7)	86.49(7)
O(22)-Mn(1)-O(1)	84.70(10)	O(19)$^{\#4}$-Mn(2)-O(7)$^{\#6}$	86.00(8)	O(3)-Mn(2)-O(7)$^{\#5}$	96.55(9)	O(22)-Mn(1)-O(7)	175.14(10)
O(15)-Mn(1)-O(1)$^{\#1}$	160.23(9)	O(19)$^{\#3}$-Mn(2)-O(19)$^{\#4}$	180.00	O(3)$^{\#2}$-Mn(2)-O(7)$^{\#5}$	83.45(9)	O(7)$^{\#5}$-Mn(2)-O(7)$^{\#6}$	180.0
O(10)-Mn(1)-O(1)$^{\#1}$	84.19(8)	O(3)-Mn(2)-O(3)$^{\#2}$	180.00				

Symmetry codes: #1 -*x*+1 ,-*y*+1, -*z*; #2 -*x*+2, -*y*, -*z*+2; #3 -*x*+2, -*y*, -*z*+1; #4 *x*, *y*, *z*+1; #5 *x*+1, *y*, *z*+1; #6 -*x*+1, -*y*, -*z*+1.

Complex **2**

Cd(1)-O(3)	2.203(3)	Cd(2)-O(10)	2.392(4)	Cd(3)-O(5)$^{\#8}$	2.259(3)	Cd(4)-O(5)$^{\#2}$	2.267(2)
Cd(1)-O(4)	2.482(3)	Cd(2)-O(11)	2.313(4)	Cd(3)-O(7)$^{\#8}$	2.401(4)	Cd(4)-O(7)$^{\#10}$	2.488(4)
Cd(1)-O(5)	2.269(3)	Cd(2)-O(11)$^{\#4}$	2.313(4)	Cd(3)-O(15)	2.229(3)	Cd(4)-O(14)$^{\#11}$	2.287(3)
Cd(1)-O(6)	2.189(4)	Cd(2)-O(12)$^{\#4}$	2.203(5)	Cd(3)-O(16)	2.347(4)	Cd(4)-O(19)	2.233(3)
Cd(1)-O(14)$^{\#3}$	2.342(3)	Cd(2)-O(12)	2.203(5)	Cd(3)-O(22)$^{\#9}$	2.735(3)	Cd(4)-O(20)	2.303(4)
Cd(1)-O(21)$^{\#2}$	2.313(3)	Cd(3)-O(4)$^{\#7}$	2.621(3)	Cd(3)-O(23)$^{\#9}$	2.261(3)	Cd(4)-O(22)$^{\#12}$	2.273(3)
Cd(2)-O(10)$^{\#4}$	2.392(4)	O(10)$^{\#4}$-Cd(2)-O(10)	114.7(2)	O(12)$^{\#4}$-Cd(2)-O(10)	83.39(17)	O(5)$^{\#8}$-Cd(3)-O(4)$^{\#7}$	115.42(9)
O(3)-Cd(1)-O(4)	76.09(11)	O(11)-Cd(2)-O(10)$^{\#4}$	93.04(14)	O(12)$^{\#4}$-Cd(2)-O(10)$^{\#4}$	148.9(2)	O(5)$^{\#8}$-Cd(3)-O(7)$^{\#8}$	87.00(12)
O(3)-Cd(1)-O(5)	109.37(1)	O(11)-Cd(2)-O(10)	54.19(13)	O(12)-Cd(2)-O(11)	102.15(19)	O(5)$^{\#8}$-Cd(3)-O(16)	161.21(11)
O(3)-Cd(1)-O(14)$^{\#3}$	89.44(11)	O(11)$^{\#4}$-Cd(2)-O(10)	93.05(14)	O(12)-Cd(2)-O(11)$^{\#4}$	117.8(2)	O(5)$^{\#8}$-Cd(3)-O(22)$^{\#9}$	93.28(10)
O(3)-Cd(1)-O(21)$^{\#2}$	94.30(13)	O(11)$^{\#4}$-Cd(2)-O(10)$^{\#4}$	54.19(13)	O(12)$^{\#4}$-Cd(2)-O(11)$^{\#4}$	102.15(19)	O(5)$^{\#8}$-Cd(3)-O(23)$^{\#9}$	90.06(11)
O(5)-Cd(1)-O(4)	174.47(1)	O(11)$^{\#4}$-Cd(2)-O(11)	121.0(2)	O(12)$^{\#4}$-Cd(2)-O(11)	117.8(2)	O(7)$^{\#8}$-Cd(3)-O(4)$^{\#7}$	155.61(13)
O(5)-Cd(1)-O(14)$^{\#3}$	99.38(9)	O(14)$^{\#11}$-Cd(4)-O(7)$^{\#10}$	96.12(11)	O(12)-Cd(2)-O(12)$^{\#4}$	93.3(2)	O(7)$^{\#8}$-Cd(3)-O(22)$^{\#9}$	73.22(11)
O(5)-Cd(1)-O(21)$^{\#2}$	95.22(11)	O(12)-Cd(2)-O(10)$^{\#4}$	83.39(17)	O(4)$^{\#7}$-Cd(3)-O(22)$^{\#9}$	112.65(9)	O(15)-Cd(3)-O(4)$^{\#7}$	78.85(11)
O(6)-Cd(1)-O(3)	152.46(1)	O(14)$^{\#11}$-Cd(4)-O(20)	166.90(11)	O(23)$^{\#9}$-Cd(3)-O(4)$^{\#7}$	68.70(11)	O(16)-Cd(3)-O(4)$^{\#7}$	82.12(13)
O(6)-Cd(1)-O(4)	76.37(13)	O(15)-Cd(3)-O(7)$^{\#8}$	87.42(12)	O(23)$^{\#9}$-Cd(3)-O(7)$^{\#8}$	123.64(12)	O(16)-Cd(3)-O(22)$^{\#9}$	72.67(11)
O(6)-Cd(1)-O(5)	98.17(13)	O(19)-Cd(4)-O(22)$^{\#12}$	90.96(11)	O(23)$^{\#9}$-Cd(3)-O(16)	90.41(13)	O(19)-Cd(4)-O(5)$^{\#2}$	88.65(10)
O(6)-Cd(1)-O(14)$^{\#3}$	86.26(14)	O(15)-Cd(3)-O(22)$^{\#9}$	154.63(11)	O(23)$^{\#9}$-Cd(3)-O(22)$^{\#9}$	50.78(10)	O(19)-Cd(4)-O(7)$^{\#10}$	170.13(13)
O(6)-Cd(1)-O(21)$^{\#2}$	82.67(16)	O(15)-Cd(3)-O(23)$^{\#9}$	147.47(12)	O(5)$^{\#2}$-Cd(4)-O(7)$^{\#10}$	99.97(11)	O(15)-Cd(3)-O(16)	87.37(13)
O(14)$^{\#3}$-Cd(1)-O(4)	81.30(10)	O(19)-Cd(4)-O(14)$^{\#11}$	88.24(10)	O(5)$^{\#2}$-Cd(4)-O(14)$^{\#11}$	92.41(9)	O(19)-Cd(4)-O(20)	101.78(13)
O(21)$^{\#2}$-Cd(1)-O(4)	83.30(11)	O(16)-Cd(3)-O(7)$^{\#8}$	77.15(15)	O(5)$^{\#2}$-Cd(4)-O(20)	96.21(11)	O(15)-Cd(3)-O(5)$^{\#8}$	102.10(11)
O(12)-Cd(2)-O(10)	148.9(2)	O(21)$^{\#2}$-Cd(1)-O(14)$^{\#3}$	162.78(11)	O(5)$^{\#2}$-Cd(4)-O(22)$^{\#12}$	178.89(12)	O(20)-Cd(4)-O(7)$^{\#10}$	72.71(13)

Symmetry codes: #2 -*x*+1, *y*, -*z*+1/2; #3 -*x*+1/2, *y*-1/2, -*z*+1/2; #4 -*x*+1, *y*, -*z*+3/2; #7 -*x*+1/2, *y*+1/2, -*z*+1/2; #8 *x*, *y*+1, *z*; #9 -*x*+1/2, -*y*+3/2, -*z*; #10 *x*+1/2, *y*-1/2, *z*; #11 -*x*+1, *y*-1, -*z*+1/2; #12 -*x*+1, -*y*, -*z*.

Complex **3**

Mn(1)-O(6)$^{\#1}$	2.227(2)	Mn(2)-O(6)$^{\#1}$	2.269(3)	Mn(2)-O(7)$^{\#1}$	2.280(3)	Mn(2)-O(3)	2.234(5)
Mn(1)-O(9)$^{\#3}$	2.145(3)	Mn(2)-O(10)$^{\#3}$	2.121(3)	Mn(2)-O(2)	2.083(3)	Mn(2)-N(1)	2.194(3)
Mn(1)-O(1)	2.125(3)	O(1)-Mn(1)-O(9)$^{\#4}$	88.06(12)	O(10)$^{\#3}$-Mn(2)-N(1)	87.69(12)	O(2)-Mn(2)-N(1)	107.30(13)
O(6)$^{\#2}$-Mn(1)-O(6)$^{\#1}$	180.00	O(1)$^{\#5}$-Mn(1)-O(9)$^{\#4}$	91.94(12)	O(2)-Mn(2)-O(6)$^{\#1}$	100.45(11)	O(3)-Mn(2)-O(6)$^{\#1}$	86.84(15)
O(9)$^{\#3}$-Mn(1)-O(6)$^{\#2}$	88.33(10)	O(1)$^{\#5}$-Mn(1)-O(1)	180.0	O(2)-Mn(2)-O(10)$^{\#3}$	95.19(14)	O(3)-Mn(2)-O(7)$^{\#1}$	84.90(15)
O(9)$^{\#3}$-Mn(1)-O(6)$^{\#1}$	91.67(10)	O(6)$^{\#1}$-Mn(2)-O(7)$^{\#1}$	57.53(9)	O(2)-Mn(2)-O(7)$^{\#1}$	156.46(12)	N(1)-Mn(2)-O(6)$^{\#1}$	151.86(11)
O(9)$^{\#3}$-Mn(1)-O(9)$^{\#4}$	180.00	O(10)$^{\#3}$-Mn(2)-O(6)$^{\#1}$	94.45(11)	O(2)-Mn(2)-O(3)	85.69(17)	N(1)-Mn(2)-O(7)$^{\#1}$	94.33(11)
O(1)-Mn(1)-O(6)$^{\#1}$	88.69(11)	O(10)$^{\#3}$-Mn(2)-O(7)$^{\#1}$	94.82(12)	O(10)$^{\#3}$-Mn(2)-N(1)	87.69(12)	N(1)-Mn(2)-O(3)	90.63(16)
O(1)-Mn(1)-O(6)$^{\#2}$	91.31(11)	O(10)$^{\#3}$-Mn(2)-O(3)	178.27(15)				

Symmetry codes: #1 -*x*+2, -*y*+1, -*z*; #2 *x*, *y*-1, *z*; #3 -*x*+1, -*y*, -*z*+1; #4 *x*+1, *y*, *z*-1; #5 -*x*+2, -*y*, -*z*.

Complex **4**

Cd(2)-O(2)$^{\#1}$	2.304(3)	Cd(2)-N(1)	2.298(4)	Cd(1)-O(3)	2.239(3)	Cd(1)-O(12)$^{\#6}$	2.363(3)
Cd(2)-O(8)$^{\#2}$	2.345(3)	Cd(2)-N(3)	2.277(3)	Cd(1)-O(4)	2.270(3)	Cd(1)-O(11)$^{\#6}$	2.471(3)
Cd(2)-O(11)$^{\#3}$	2.355(3)	Cd(2)-O(5A)	2.31(2)	Cd(1)-O(8)$^{\#5}$	2.446(3)	Cd(1)-O(9)$^{\#5}$	2.401(3)
Cd(2)-O(5)	2.211(19)	Cd(1)-O(6)	2.318(4)	O(3)-Cd(1)-O(4)	81.78(12)	O(4)-Cd(1)-O(6)	93.17(13)
O(2)$^{\#1}$-Cd(2)-O(8)$^{\#2}$	90.49(13)	N(1)-Cd(2)-O(8)$^{\#2}$	90.60(12)	O(3)-Cd(1)-O(8)$^{\#5}$	100.84(12)	O(8)$^{\#5}$-Cd(1)-O(11)$^{\#6}$	71.63(11)
O(3)-Cd(1)-O(6)	174.93(1)	N(1)-Cd(2)-O(11)$^{\#3}$	163.01(12)	O(3)-Cd(1)-O(12)$^{\#6}$	89.50(13)	O(12)$^{\#6}$-Cd(1)-O(8)$^{\#5}$	124.97(11)
O(2)$^{\#1}$-Cd(2)-O(5A)	168.0(6)	N(1)-Cd(2)-O(5A)	107.7(7)	O(3)-Cd(1)-O(11)$^{\#6}$	92.73(12)	O(6)-Cd(1)-O(9)$^{\#5}$	85.95(14)
N(3)-Cd(2)-O(2)$^{\#1}$	85.38(13)	O(12)$^{\#6}$-Cd(1)-O(11)$^{\#6}$	53.84(11)	O(3)-Cd(1)-O(9)$^{\#5}$	94.66(13)	O(12)$^{\#6}$-Cd(1)-O(9)$^{\#5}$	175.77(13)
O(5)-Cd(2)-O(2)$^{\#1}$	166.6(6)	N(3)-Cd(2)-O(8)$^{\#2}$	172.73(12)	O(2)$^{\#1}$-Cd(2)-O(11)$^{\#3}$	86.42(12)	O(9)$^{\#5}$-Cd(1)-O(8)$^{\#5}$	53.44(11)
O(5)-Cd(2)-O(8)$^{\#2}$	76.3(5)	N(3)-Cd(2)-O(11)$^{\#3}$	98.24(13)	O(4)-Cd(1)-O(8)$^{\#5}$	145.92(11)	O(9)$^{\#5}$-Cd(1)-O(11)$^{\#6}$	125.01(11)
O(5)-Cd(2)-O(11)$^{\#3}$	92.2(8)	N(3)-Cd(2)-N(1)	94.90(14)	O(4)-Cd(1)-O(12)$^{\#6}$	88.83(12)	O(6)-Cd(1)-O(8)$^{\#5}$	83.58(13)
O(5)-Cd(2)-N(1)	94.0(9)	N(3)-Cd(2)-O(5A)	96.3(9)	O(4)-Cd(1)-O(11)$^{\#6}$	142.44(12)	O(6)-Cd(1)-O(12)$^{\#6}$	89.97(14)
O(5)-Cd(2)-N(3)	108.0(6)	O(5A)-Cd(2)-O(8)$^{\#2}$	86.5(8)	O(4)-Cd(1)-O(9)$^{\#5}$	92.53(12)	O(6)-Cd(1)-O(11)$^{\#6}$	91.03(13)
N(1)-Cd(2)-O(2)$^{\#1}$	83.94(12)	O(5A)-Cd(2)-O(11)$^{\#3}$	81.6(6)	O(8)$^{\#2}$-Cd(2)-O(11)$^{\#3}$	75.50(12)		

Symmetry codes: #1 *x*, -*y*+1, *z*+1/2; #2 *x*+1/2, -*y*+1/2, *z*+1/2; #3 *x*+1/2, -*y*+3/2, *z*+1/2; #4 *x*, -*y*+1, *z*-1/2; #5 *x*+1/2, *y*+1/2, *z*; #6 *x*+1/2, *y*-1/2, *z*.